Journal of Applied Electrochemistry (2006) 36:531–538
DOI 10.1007/s10800-005-9075-x


# Underpotential deposition of Tl on Ag in the presence of bromide ions – Estimation of specific capacitance for design of electrochemical supercapacitors

T.C. GIRIJA and M.V. SANGARANARAYANAN*
*Department of Chemistry, Indian Institute of Technology, Madras 600 036, India*
*(*author for correspondence, e-mail: sangara@iitm.ac.in)*

Received 19 January 2005; accepted in revised form 8 September 2005

*Key words:* cyclic voltammetry, electrochemical supercapacitors, galvanostatic charge/discharge, impedance spectroscopy, thallium, underpotential deposition

**Abstract**

The analysis of underpotential deposition (UPD)-based systems for the development of electrochemical supercapacitors is investigated employing the UPD of Tl on Ag in the presence of bromide ions, as an illustrative example. The specific capacitance is estimated with the help of multi-cycle voltammograms, galvanostatic charge/discharge experiments and impedance spectroscopy. The equivalent circuit for the system is constructed and the parameters are deduced from the simulation. The deduced magnitude of $\sim 10^2$ F $g^{-1}$ in conjunction with the satisfactory number of charge/discharge cycles obtained from Galvanostatic experiments indicate the feasibility of these systems as supercapacitors.

## 1. Introduction

The search for suitable electrochemical supercapacitors which possess large specific capacitance and long cycle life has been intensified during the past few decades, on account of the market demand for high power devices [1]. Among a variety of systems investigated in this context, mention may be made of the following [2]: (i) activated carbon under different pre-treatment protocols; (ii) Ruthenium dioxide in acidic environments; and (iii) conducting polymer-based systems. The essential motivation behind such multi-faceted attempts lies in the trade-off required among various competitive target parameters viz. satisfactory charge/discharge behaviour; inexpensive nature of the materials, ease of processability vis-a-vis fabrication and high specific capacitances.

Conventional capacitors [3] consisting of two metal sheets on either side of the dielectric materials, make use of the low dielectric constant in conjunction with small thickness and large plate area. In electrolytic capacitors, however, only one of its conducting surfaces is a metallic plate, the other conducting surface being a chemical compound or electrolyte. In contrast, the electrochemical supercapacitor exploits the non-Faradaic (electrical double layer) as well as Faradaic (charge transfer) processes in order to obtain enhanced capacitances. Recalling that the thickness of the electrical double layer is ca. 3 Å, the origin of extremely high values for capacitance is obvious. Furthermore, reversible charge transfer processes constituting the pseudocapacitance ensure that the reversibility behaviour of capacitors is maintained. These two salient features viz. $\sim 10^{-8}$ cm as the double layer thickness and reversible Faradaic processes over a wide potential window point to the feasibility of developing supercapacitors with desirable operational characteristics. Although early investigations in the design and development of supercapacitors were essentially concerned with obtaining large capacitances ca. $10^2$ F $g^{-1}$ of the material, recent studies focus on the charge/discharge characteristics, device applications and lowering the cost of materials.

Apart from double-layer capacitances, the Faradaic charge transfer processes also contribute to the capacitance and this contribution is termed pseudocapacitance [4]. Among several contexts wherein the pseudocapacitance arises, mention may be made of the following [4]: (a) underpotential deposition (UPD) of metals and adatoms on different substrates viz. H or Cu on Pt, Pb on Au, Bi on Ag, H on Rh or Pt; (b) redox processes wherein the electrode potential varies with the activities of the components; and (c) chemisorption at electrochemical interfaces with potential-dependent partial charge transfer.

The phenomenon of UPD indicates the onset of deposition of adatoms at different substrates in potential ranges positive to the reversible Nernst potential. UPD-based supercapacitor systems are favourable in view of (i) high reversibility; (ii) large pseudocapacitance

values; (iii) the wide choice of the substrate and depositing species; (iv) feasibility of employing aqueous and non-aqueous solvents; (v) specific choice of electrolytes in order to increase adsorption via pseudocapacitance; and (vi) manipulation of the potential window as dictated by the objective under consideration.

The voltammetric behaviour of the UPD of Tl on Ag has been studied extensively during the past few decades on various electrocatalytic processes such as reduction of $O_2$ [5], reduction of $Fe^{3+}$, $Ce^{4+}$ and $S_2O_8^{2-}$ and *p*-benzoquinone [6, 7]. The effect of halide anions on the UPD of Tl on Ag has also been studied using various electrochemical, radiotracer, optical, *in situ* STM techniques [8–11]. The addition of anions in the study of UPD of Tl on Ag decreases the UPD shift as well as increases the surface charge densities [12], which is reflected in the large area under the voltammetric peak. This arises since the adsorption of metal adatoms is accompanied by desorption of halide ions, both processes contributing to the current and thereby producing a larger surface charge, which subsequently leads to higher pseudocapacitance values. The amount of adsorption among halides varies as $F^- < Cl^- < Br^- < I^-$. The study of UPD of Tl in the presence of $I^-$ is precluded in view of its instantaneous precipitation in aqueous solutions. Consequently, it is instructive to investigate whether the underpotentially deposited Tl on Ag in the presence of $Br^-$ ions would be suitable for developing supercapacitors.

The objectives of this communication are (i) to demonstrate the feasibility of UPD-based systems as supercapacitors using an illustrative example of Tl on Ag in the presence of $Br^-$ ions; (ii) to estimate the specific capacitance of UPD-based supercapacitors employing voltammetric and galvanostatic charge/discharge studies; and (iii) to deduce the low and high frequency components of the capacitance using impedance analysis.

## 2. Experimental

Electrochemical measurements were carried out in a three-electrode cell consisting of a polycrystalline Ag electrode (Bio Analytical Systems, USA) of 1.6 mm diameter as the working electrode, Pt foil counter electrode (Bio Analytical Systems, USA) and Ag/AgCl electrode (Bioanalytical systems, USA) as the reference electrode. Before each experiment, the working electrode was polished with alumina solution on alumina pads. Analar grade $KNO_3$ was used as received and employed as the supporting electrolyte. Analar grade $TlNO_3$ and KBr (Fluka Chemicals, India) were used as received. Cyclic voltammetry, galvanostatic charge/discharge and impedance analysis were performed using an electrochemical workstation, CHI 660A (CH Instruments, USA). Impedance measurements were recorded in the frequency range $10^5$ Hz to 10 Hz with an amplitude of 5 mV. All experiments were carried out at a temperature of 25 ± 1 °C.

## 3. Results and discussion

### 3.1. *Cyclic voltammetric studies*

Cyclic voltammetric studies were carried out in order to determine the influence of control variables such as sweep rate, number of cycles, etc on the UPD of Tl on Ag in the presence of $Br^-$ions. Figure 1 displays the current–potential response for the UPD of Tl on Ag in the presence of $Br^-$ ions (in 2 mM $TlNO_3$ + 20 mM KBr + 1M $KNO_3$ solution) at a scan rate of 0.1 V $s^{-1}$. The cathodic and anodic peaks at −0.56 V and −0.52 V are attributed respectively to the underpotential deposition and dissolution of Tl on Ag. The peaks at −0.68 V and −0.82 V are attributed to the bulk deposition and stripping of Tl. The underpotential deposition/dissolution peaks of Tl on Ag obtained here are consistent with those reported in the literature [13, 14]. As can be seen from Figure 1, the reversibility was maintained upto 1000 cycles. The present study thus exploits the high reversibility property of UPD of Tl on Ag and demonstrates the feasibility of UPD of Tl on Ag in the presence of $Br^-$ ions as a candidate for the design of supercapacitors. The notion of reversibility in the present context denotes the constancy of the peak potential even at very high scan rates. In the present investigation, the UPD peak potentials remain constant (∼−0.57 V) at scan rates ranging from 0.1 V $s^{-1}$ to 10 V $s^{-1}$; further the difference in the peak potentials for UPD and stripping is constant. The underpotential deposition/stripping peaks are symmetric and hence they are referred to as 'mirror images' (Figure 3) whereas the bulk deposition/dissolution peaks are non-symmetric. Hence the term "mirror image" refers only to the underpotential deposition and stripping region. Although the reduction of nitrate ions is expected to occur in the potential region of interest, an appreciable current is not noticed (cf. Figure 1 for the blank cyclic voltammogram) at the scan rate employed by us. Further this current affects the charge to an extent of ∼1%.

Figure 2 depicts the analogous current–potential data at a scan rate of 1.0 V $s^{-1}$ and the response remains essentially reversible up to 1000 cycles even at a high scan rate. The current–potential response at various scan rates from 0.5 V $s^{-1}$ to 2.0 V $s^{-1}$ is shown in Figure 3 and the reversibility is maintained at all scan rates. The reversibility behaviour of UPD of Tl on Ag has been emphasized by Tang and Furtak [15] and it was demonstrated that among the three UPD systems studied on Ag using an electrochemical quartz crystal microbalance (EQCM) viz. Cd, Tl and Pb, the UPD of Tl shows mirror images ensuring higher reversibility. In the underpotential deposition of Tl on Ag in the presence of $Br^-$ ions, two effects arise, the first being a decrease in the underpotential shift due to a reduction in bond strength between the metal adatom and the substrate surface arising from the interaction of $Br^-$ ions with the substrate, which is stronger than the Tl–Ag interaction; the second effect leads to an increase in surface charge due to the adsorption of Tl adatoms and desorption of

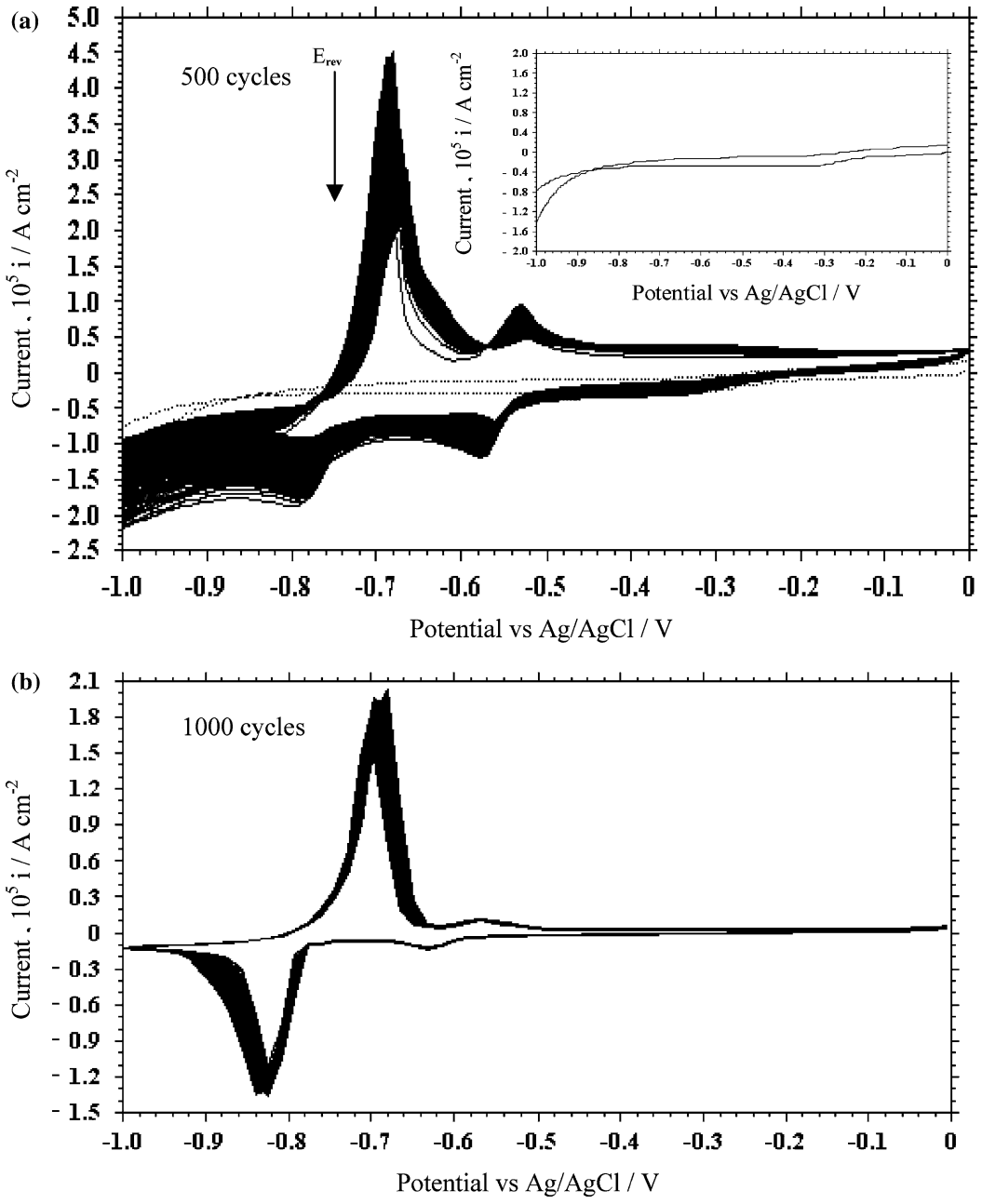


*Fig. 1.* Multi-cycle voltammogram of UPD of Tl on Ag in the presence of $Br^-$ ions at a scan rate of 0.1 V $s^{-1}$. Electrolyte solution consists of 2 mM $TlNO_3$ + 20 mM KBr + 1M $KNO_3$. $E_{rev}$ denotes the reversible Nernst potential for $Tl^+$/Tl couple. Inset depicts the cyclic voltammogram of Ag in 1 M $KNO_3$.

$Br^-$ ions. These two effects yield higher charges for UPD systems in the presence of bromide ions.

### 3.2. *Galvanostatic charge/discharge experiments*

In order to further ascertain the feasibility of the UPD system of Tl on Ag in the presence of $Br^-$ ions as a supercapacitor, galvanostatic charge/discharge experiments were carried out. A typical chronopotentiogram obtained at a constant current density of 10.0 $\mu$A cm$^{-2}$ over a potential range of −0.6 V (region of UPD) is shown in Figure 4. This demonstrates the customary charging/discharging behaviour (ideally a 'Λ Λ Λ ....' shaped voltage response) exhibited by other supercapacitors too [16, 17]. Furthermore, the charge curves are symmetrical to their corresponding discharge counterparts in the potential region of investigation – an essential criterion for the feasibility of supercapacitors.

### 3.3. *Evaluation of specific capacitance*

#### 3.3.1. *From cyclic voltammetry*

The pseudocapacitance is estimated using the voltammetric charges on either positive or negative sweeps of a cyclic voltammogram in an inert electrolyte [18]. In our present analysis, the pseudocapacitance ($C_q$*) is estimated using the following equation

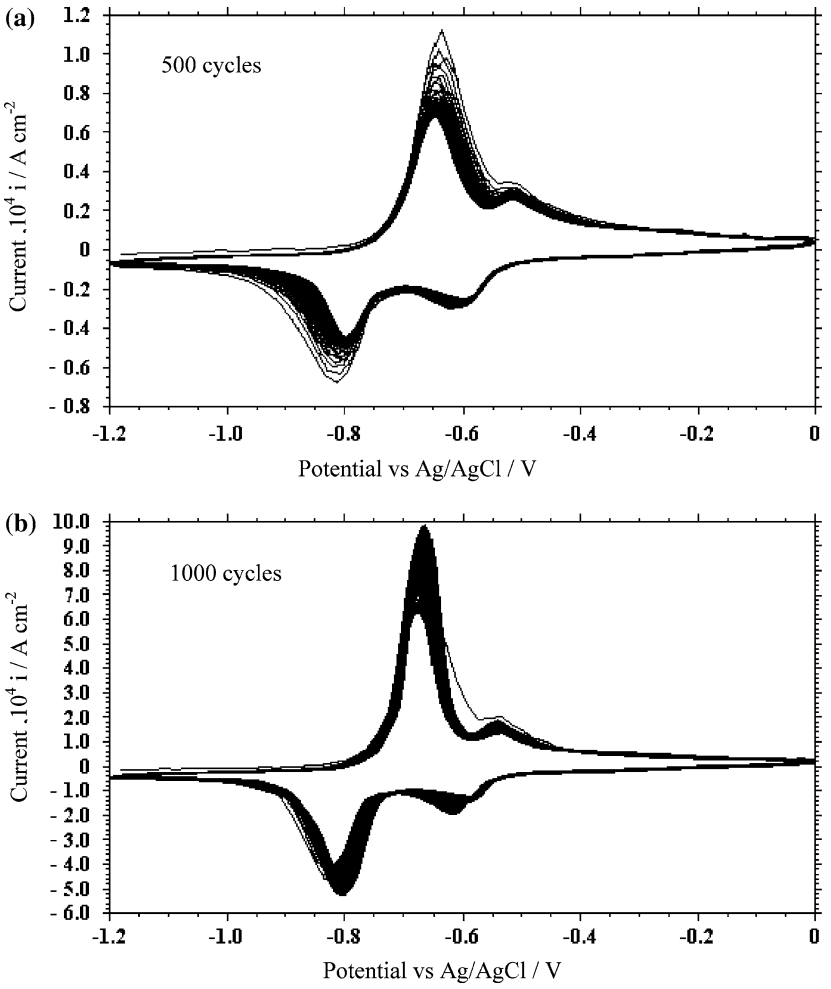


*Fig. 2.* Multi-cycle voltammogram of UPD of Tl on Ag in the presence of $Br^-$ ions at a scan rate of 1.0 V $s^{-1}$. Electrolyte solution consists of 2 mM $TlNO_3$ + 20 mM KBr + 1M $KNO_3$.

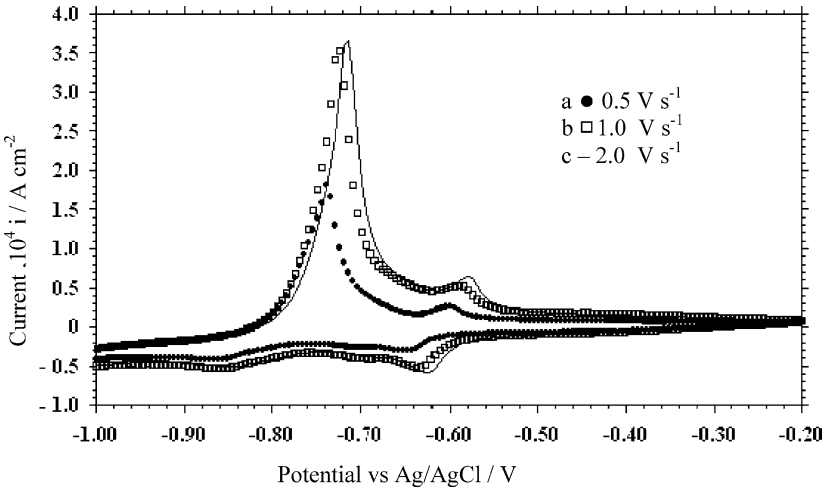


*Fig. 3* Cyclic voltammograms of UPD of Tl on Ag in the presence of $Br^-$ ions at various scan rates. Electrolyte solution consists of 2 mM $TlNO_3$ + 20 mM KBr + 1M $KNO_3$.

$$C_{q*} = q^*/\Delta V \qquad (1)$$

where $q^*$ and $\Delta V$ represent the charge density and potential range, respectively. Accordingly, the cathodic voltammetric charge density ($q^*$) obtained by the integration of the cyclic voltammogram from −1.0 to 0 V of Figure 1a at a scan rate of 0.1 V $s^{-1}$ is $8.12 \times 10^{-5}$ C $cm^{-2}$. The potential range ($\Delta V$) employed

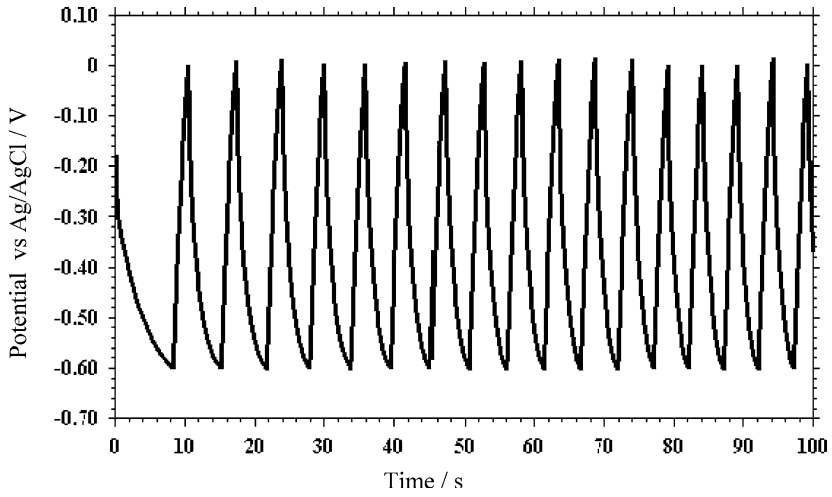


*Fig. 4.* Galvanostatic charge/discharge curves of Tl UPD on Ag in the presence of $Br^-$ ions at a current density of 10.0 $\mu$A cm$^{-2}$. Electrolyte solution consists of 2 mM $TlNO_3$ + 20 mM KBr + 1M $KNO_3$.

is 1.0 V, thus yielding the pseudocapacitance as $8.12 \times 10^{-5}$ F cm$^{-2}$. In order to obtain the specific capacitance per unit weight of the material, the active area of Ag is required. The geometrical area of the Ag electrode employed is $2.01 \times 10^{-2}$ cm$^2$. Since the roughness factor for Ag [19] surface is ca. 1.5, the electrochemical surface area is $3.014 \times 10^{-2}$ cm$^2$. The number of atoms of Ag corresponding to this area is given as electrochemical area/(interatomic distance)$^2$. Assuming the interatomic distance in Ag atoms as 2.5 Å, the number of Ag atoms is $4.8 \times 10^{13}$, the number of moles being $8.01 \times 10^{-11}$. This yields $2.87 \times 10^{-7}$ g cm$^{-2}$ as the active weight per unit area and consequently, the specific capacitance is deduced as $2.82 \times 10^2$ F g$^{-1}$. For other scan rates, the same procedure yields the specific capacitance values reported in Table 1.

### 3.3.2. *From galvanostatic charge/discharge experiments*

The pseudocapacitance may also be evaluated from galvanostatic charge/discharge experiments as [20]

$$C_{cp} = i\Delta t/\Delta v \times m \quad (2)$$

where $i$, $\Delta t$, $\Delta v$ and $m$ denote respectively current density, discharge time, potential range and the active weight of the electrode material. The values of specific capacitances (in F g$^{-1}$) are obtained as $2.40 \times 10^2$, $1.30 \times 10^2$ and $1.27 \times 10^2$ respectively at the current densities of 10.0, 50.0 and 75.0 $\mu$A cm$^{-2}$. The specific capacitance estimated from cyclic voltammogram ($2.82 \times 10^2$ F g$^{-1}$) in good agreement with that obtained from charge/discharge experiments at 10.0 $\mu$A cm$^{-2}$ ($2.40 \times 10^2$ F g$^{-1}$). The variation of the specific capacitance with the number of charge/discharge cycles is shown in Figure 5. In comparison with an initial capacitance of ~240 F g$^{-1}$ (at 10.0 $\mu$A cm$^{-2}$), the capacitance after 100 cycles becomes ~235 F g$^{-1}$ suggesting that there is no appreciable decrease with the number of cycles. However, when the current density is increased to 75.0 $\mu$A cm$^{-2}$, the specific capacitance decreases from ~127 F g$^{-1}$ to ~108 F g$^{-1}$.

*Table 1.* Specific capacitance obtained from different experimental methods for the underpotential deposition of Tl on Ag in the presence of bromide ions

| Experimental technique | Parameter | $10^2$ specific capacitance (F g$^{-1}$) |
|---|---|---|
| Cyclic voltammetry | Scan rate (V s$^{-1}$) | |
| | 0.1 | 2.82 |
| | 0.5 | 2.02 |
| | 1.0 | 1.64 |
| | 2.0 | 1.12 |
| Galvanostatic charge/discharge | Current density ($\mu$A cm$^{-2}$) | |
| | 10.0 | 2.40 |
| | 50.0 | 1.30 |
| | 75.0 | 1.25 |
| Impedance spectroscopy | Potential (V) | |
| | −0.50 | 0.80 |
| | −0.65 | 1.20 |

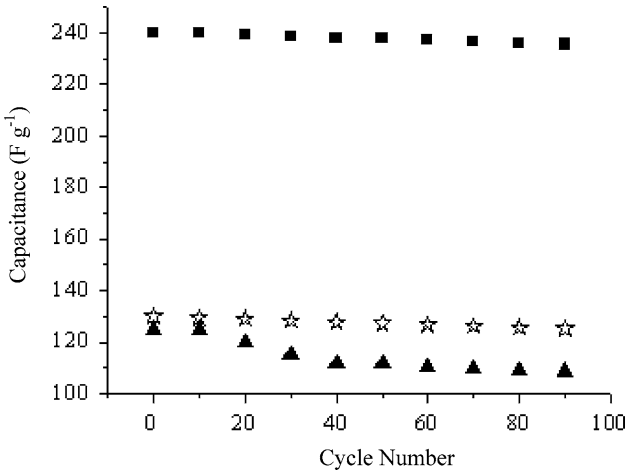


*Fig. 5.* Variation of capacitance with the number of cycles at various current densities, ■ 10 $\mu$A cm$^{-2}$, ☆ 50 $\mu$A cm$^{-2}$ and ▲ 75 $\mu$A cm$^{-2}$.

### 3.4. *Impedance studies*

Figure 6 shows the complex plane (Nyquist) plots of the impedance of UPD of Tl on Ag in the presence of $Br^-$ ions at various underpotentials viz. −0.25 to −0.65 V. Each plot is characterized by a depressed semi-circle in the high frequency region and a vertical line whose slope is less than unity. The low-frequency differential capacitance ($C_t$) [21] can be calculated from the variation of the imaginary component of the impedance with the reciprocal of the frequency ($-Z''$ vs. $1/f$). The slope of this plot (Figure 7) is equal to $1/(2\pi C_t)$ and for the potential range between −0.25 V and −0.65 V, $-Z''$ vs. $1/f$ plots exhibit a linear correlation. The capacitance values (in F $g^{-1}$) at −0.25 and −0.65 V (regions of UPD) are $0.8\times10^2$ and $1.2 \times 10^2$, respectively. These values are in general agreement with those obtained from charge/discharge experiments.

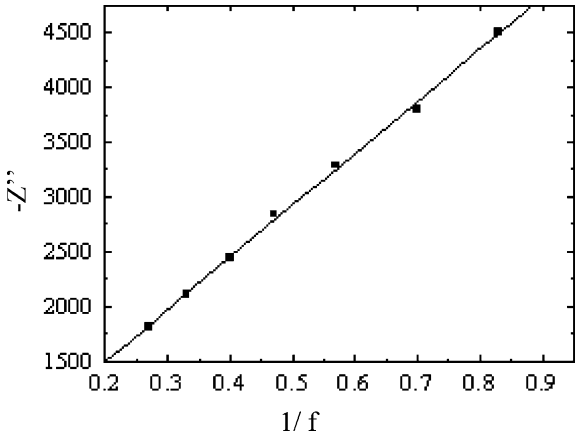


*Fig. 7.* Variation of imaginary component of impedance ($-Z''$) with reciprocal of frequency ($1/f$) at −0.65 V. Points denote the experimental data while the line is obtained from the linear regression analysis. Correlation coefficient ~0.99.

A plausible equivalent circuit which is in accordance with the above Nyquist plot is shown in Figure 8. In this model, the double layer capacity and the Warburg impedance for semi-infinite linear diffusion are replaced by two constant phase elements (CPEs). Similar equivalent circuits have been proposed earlier in related contexts wherein depressed semi-circles are noticed [14]. The two constant phase elements $CPE_1$ and $CPE_2$ incorporate, respectively, the distribution of double layer capacity and the variation in the diffusion coefficients arising on account of the inhomogeneous nature of the electrode surface. The incorporation of CPE becomes essential on account of the roughened Ag surface – a consequence of the electrode pre-treatment procedures employed. Thus, the double layer capacity

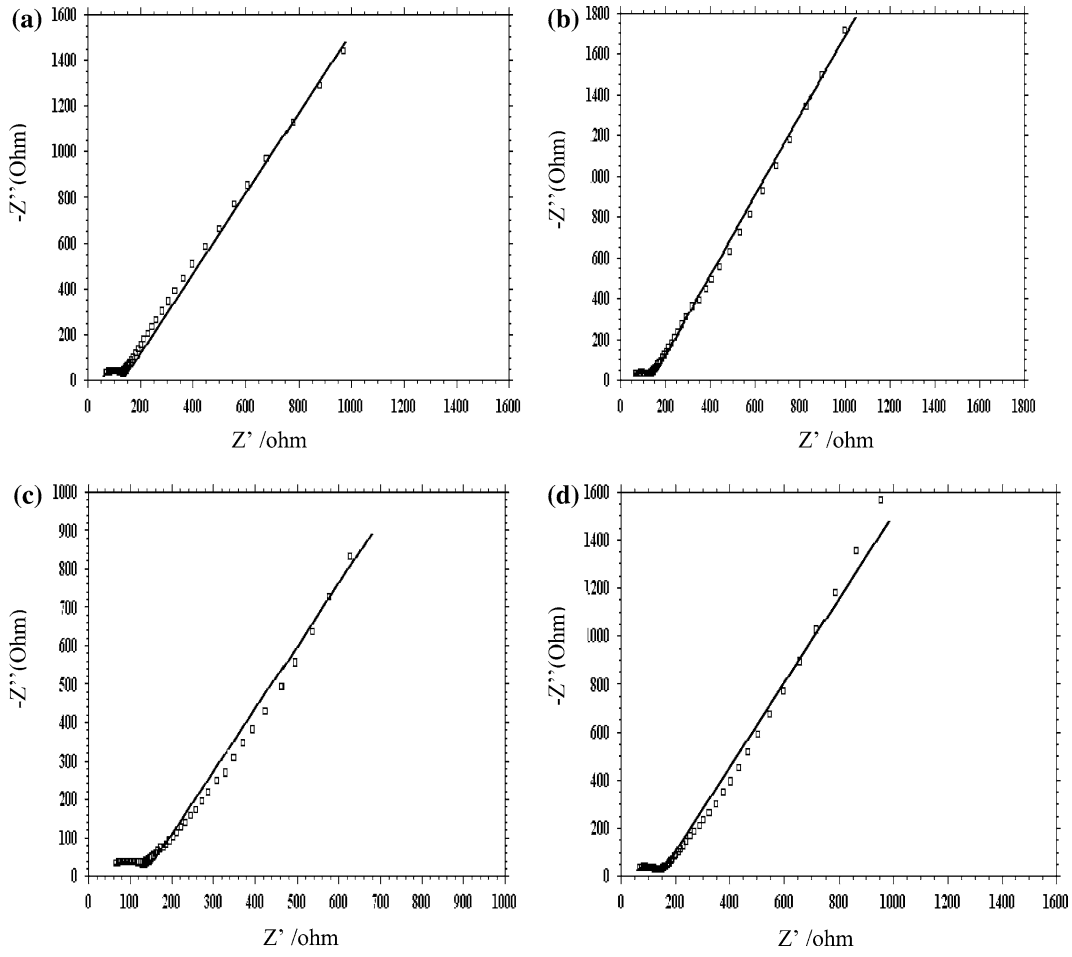


*Fig. 6.* Nyquist plot of UPD of Tl on Ag in the presence of $Br^-$ ions. Frequency range: $10^5$ Hz–1 Hz. Squares denote experimental values while the line represents the fitting of the data to the equivalent circuit of Figure 8.

*Table 2.* Equivalent circuit parameters deduced by fitting the Nyquist plots to the circuit of Figure 8.

| S. No | Applied potential vs. Ag/AgCl (V) | $R_{ct}$ (ohm cm$^2$) | $10^{-7}$ $CPE_1$ (ohm$^{-1}$ cm$^{-2}$ s) | $10^{-4}$ $CPE_2$ (ohm$^{-1}$ cm$^{-2}$ s) | $n_1$ | $n_2$ |
|---|---|---|---|---|---|---|
| 1. | −0.25 | 90 ± 0.5 | 8.3 ± 0.1 | 1.5 ± 0.2 | 0.79 ± 0.05 | 0.90 ± 0.01 |
| 2. | −0.4 | 92 ± 1 | 8.5 ± 0.1 | 1.2 ± 0.2 | 0.78 ± 0.02 | 0.92 ± 0.02 |
| 3. | −0.5 | 94 ± 0.4 | 8.9 ± 0.2 | 1.2 ± 0.3 | 0.76 ± 0.01 | 0.94 ± 0.01 |
| 4. | −0.65 | 97 ± 0.5 | 8.3 ± 0.1 | 1.2 ± 0.1 | 0.67 ± 0.01 | 0.97 ± 0.01 |

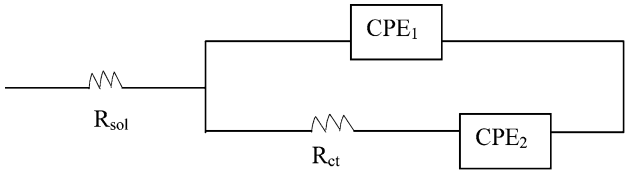


*Fig. 8.* Equivalent circuit for UPD of Tl on Ag in the presence of $Br^-$ ions. $R_{sol}$, electrolyte resistance; $R_{ct}$, charge transfer resistance; $CPE_1$ and $CPE_2$ denote constant phase elements.

and Warburg impedance, customarily introduced in the Randles circuit, are replaced by the constant phase elements. In general, the appearance of a CPE may arise from (a) a distribution of the relaxation times due to inhomogenities existing at the electrode/electrolyte interface; (b) porosity; (c) nature of the electrode; and (d) dynamic disorder associated with diffusion. The fitting of the equivalent circuit has been carried out using the AC impedance simulator of the electrochemical workstation. The solution resistance obtained from the fitting procedure is found to be 43 ± 1 ohm cm$^2$.

The impedance of the two constant phase elements are defined as $Z_{CPE_1} = [Q(j\omega)^{n_1}]^{-1}$ and $Z_{CPE_2} = [Q(j\omega)^{n_2}]^{-1}$ with each exponent lying in the range −1 to +1. The parameter $Q$ consists of properties related to the surface and the electroactive species, ω is the angular frequency ($\omega = 2\pi f$) while the exponent $n$ arises from the slope of the log $Z$ vs. log $f$ plot. In general, the slope of log $Z$ vs. log $f$ plot (denoted as $n$) is a manifestation of the electrode nature. A pure capacitance yields $n = 1$, a pure resistance yields $n = 0$, while $n = 0.5$ represents the Warburg impedance. From Table 2, it follows that in the potential range of −0.25 to −0.65 the value of $n_1$ deduced as ∼0.7 refers to the inhomogeneous nature of the Ag electrode while the value of $n_2$ equals ∼0.8 at −0.65 V (the potential at which UPD is complete). The increase in the value of $R_{ct}$ from −0.20 V to −0.65 V indicates an enhancement in the surface coverage of thallium adatoms and $Br^-$. However, a clear delineation arising from each adsorbed species requires a model for competitive adsorption and will be discussed in a future communication.

Table 1 denotes the specific capacitances obtained from different experimental methods for the present system. As seen from the Table 1, specific capacitances deduced from the UPD-based systems in the presence of anions compare favourably with those based on conducting polymers viz polypyrrole [22], polyaniline [23], poly(ethylenedioxythiophene) (PEDOT) [24], etc as well as carbon nanotubes [25]. Although the metal oxide-based supercapacitors offer a higher capacitance (∼750.0 F g$^{-1}$), they are not cost effective. Hence, UPD-based systems can become potential candidates for supercapacitors. Nevertheless, the precise influence of larger scan rates, the nature of the substrate employed vis-a-vis depositing species and the maximum specific capacitance attainable for UPD-based systems need further study.

## 4. Summary

The feasibility of UPD-based systems for development of supercapacitors is demonstrated with the help of multi-cycle voltammetric, galvanostatic charge/discharge and impedance studies. Specific capacitance values of $10^2$ F g$^{-1}$ are shown to arise from the UPD of Tl on Ag in the presence of $Br^-$ ions. The charge/discharge experiments indicate that the reversibility is maintained for $\sim 10^2$ cycles.

## Acknowledgements

The valuable comments of the reviewer are gratefully acknowledged. The financial support by DRDO, Government of India is gratefully acknowledged.

## References

1. A. Burke, *J. Power Sources* **91** (2000) 37.
2. S. Sarangapani, B.V. Tilak and C.P. Chen, *J. Electrochem. Soc.* **143** (1996) 3791.
3. B.E. Conway, *Electrochemical Supercapacitors: Scientific Fundamentals Technological Applications* (Kluwer Academic Publishers/Plenum Press, New York, 1999).
4. B.E. Conway, V. Birss and J. Wojtowicz, *J. Power Sources* **66** (1997) 14.
5. A. Zwetanova and K. Juttner, *J. Electroanal. Chem.* **119** (1981) 149.
6. A.M. Abd El-Halim, K. Juttner and W.J. Lorenz, *J. Electroanal. Chem.* **106** (1980) 193.
7. C. Mayer, K. Juttner and W.J. Lorenz, *J. Appl. Electrochem.* **9** (1979) 161.
8. B.W. Mao, Z.Q. Tian and M. Fleischmann, *Electrochim. Acta* **37** (1992) 1767.
9. P. Waszcsuk, A. Wnuk and J. Sobkowski, *Electrochim. Acta* **44** (1999) 1789.
10. A. Bewick and B. Thomas, *J. Electroanal. Chem.* **65** (1975) 911.
11. D. Carnal, P.I. Oden, U. Muller, E. Schmidt and H. Siegenthaler, *Electrochim. Acta* **40** (1995) 1223.

12. D.M. Kolb. *in* H. Gerischer and C.W. Tobias (Eds), Advances in Electrochemistry and Electrochemical Engineering 11, (John Wiley Interscience, New York, 1978), pp. 177–178.
13. V. Daujotis and E. Gaidamauskas, *J. Electroanal. Chem.* **446** (1998) 151.
14. T.C. Girija and M.V. Sangaranarayanan, *J. Colloid Interf. Sci.* **282** (2005) 92.
15. Y. Tang and T.E. Furtak, *Electrochim. Acta* **36** (1991) 1869.
16. Chi-Chang Hu and Chen-Ching Wang, *Electrochem. Commun.* **4** (2002) 554.
17. A.K. Chatterjee, M. Sharon, R. Banerjee and M. Neumann-Spallart, *Electrochim. Acta* **48** (2003) 3439.
18. Chi-Chang Hu and Kwang-Huei Chang, *J. Power Sources* **112** (2002) 401.
19. A.J. Motheo, S.A.S. Machado, M.H. Van Kampen and J.R. Santos Jr., *J. Braz. Chem. Soc.* **4** (1993) 122.
20. Wei-Chih Chen and Ten-Chin Wen, *J. Power Sources* **117** (2003) 273.
21. D. Belanger, X. Ren, J. Davey, F. Uribe and S. Gottesfeld, *J. Electrochem. Soc.* **147** (2000) 2923.
22. M.D. Ingram, H. Staesche and K.S. Ryder, *J. Power Sources* **129** (2002) 107.
23. J.M. Ko, R.Y. Song, H.J. Yu, J.W. Yoon, B.G. Min and D.W. Kim, *Electrochim. Acta* **50** (2004) 868.
24. Kwang Sun Ryu, Young-Gi Lee, Young-Sik Hong, Yong Joon Park, Xianlan Wu, Kwang Man Kim, Man Gu Kang, Nam-Gyu Park and Soon Ho Chang, *Electrochim. Acta* **50** (2004) 838.
25. E. Frackowiak, S. Delpeux, K. Jurewicz, K. Szostak, D. Cazorla-Amoros and F. Béguin, *Chem. Phys. Lett.* **361** (2002) 35.